Optimization of Modulation Waveforms for Improved EMI Attenuation in Switching Frequency Modulated Power Converters

Deniss STEPINS[1], *Jin HUANG*[2]

[1]Institute of Radio Electronics, Faculty of Electronics and Telecommunications, Riga Technical University, 16 Azenes Street, LV-1048 Riga, Latvia
[2]School of Electrical and Electronic Engineering, Huazhong University of Science and Technology, 1037 Luoyu Road, Wuhan 430074, China

deniss.stepins@rtu.lv, huangjin.mail@163.com

DOI: 10.15598/aeee.v13i1.1142

Abstract. *Electromagnetic interference (EMI) is one of the major problems of switching power converters. This paper is devoted to switching frequency modulation used for conducted EMI suppression in switching power converters. Comprehensive theoretical analysis of switching power converter conducted EMI spectrum and EMI attenuation due the use of traditional ramp and multislope ramp modulation waveforms is presented. Expressions to calculate EMI spectrum and attenuation are derived. Optimization procedure of the multislope ramp modulation waveform is proposed to get maximum benefits from switching frequency modulation for EMI reduction. Experimental verification is also performed to prove that the optimized multislope ramp modulation waveform is very useful solution for effective EMI reduction in switching power converters.*

Keywords

Electromagnetic interference, frequency modulation, optimization, switching power converter.

1. Introduction

Switching power converters (SPC) used in many electronic devices for electric power conversion are noticeable sources of electromagnetic interference (EMI) which can deteriorate normal operation of other electronic equipment. EMI both conducted and radiated must be reduced in order to meet international electromagnetic compatibility standards (e.g. CISPR 22) requirements. Traditional ways for conducted EMI reduction usually are input EMI filters, proper design of printed circuit boards, soft-switching techniques, etc. Recently two more novel conducted EMI reduction techniques have been proposed and used [1], [2], [3], [4], [5]. The first one is active EMI filtering using digital signal processing [4] and the second one is spread spectrum technique [3]. The spread spectrum technique which is usually based on switching frequency modulation (SFM) is very attractive technique mainly because it is simple to implement. By modulating the switching frequency peak conducted EMI levels can be easily suppressed using simple periodic modulation waveforms (such as sine, triangle, sawtooth, etc) as shown in Fig. 3. The main parameters of periodic SFM are switching frequency deviation Δf_{sw}, modulation frequency f_m and modulating waveform $m(t)$ with unitary amplitude. Of course, for modulating the switching frequency random and chaotic signals can be used, but the use of simple periodic modulation waveforms is more popular in practical SPC, mainly because negative effect of periodic SFM on peak-to-peak output voltage ripples is less visible and periodic SFM is simpler to implement than random or chaotic SFM [6], [7].

Benefits of periodic SFM for EMI reduction can be significantly reduced due to amplitude modulation of SPC currents caused by SFM [8]. The amplitude modulation leads to EMI spectrum sidebands distortion and asymmetry with respect to central switching frequency f_{sw0} and consequently EMI attenuation is lower than expected for the given value of modulation index [8], [9]. In order to increase effectiveness of SFM for EMI reduction in SPC (especially for higher values of Δf_{sw}), multislope ramp modulating waveform (MRMW) was proposed by S. Johnson and R. Zane [8].

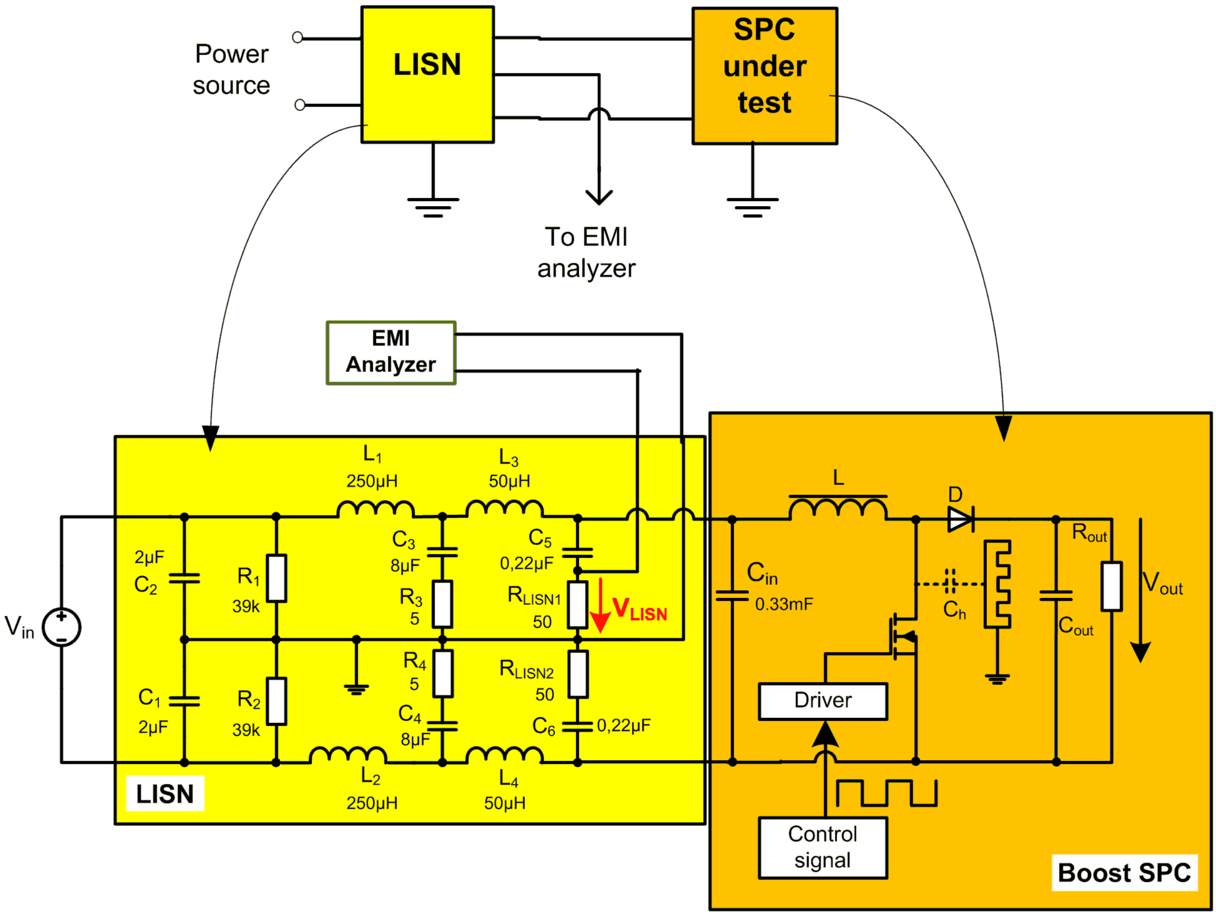

Fig. 1: Typical conducted EMI measurement setup (top) and boost SPC schematic diagram with LISN (bottom) used in the analysis.

Slopes of the MRMW are set by parameter t_0 (Fig. 5). As it is stated in [8], electronic ballast output current spectral distortion and output EMI can be effectively reduced when $t_0 = 0.35T_m$ (where T_m is modulation period). However as it will be proved in our paper, t_0 is the function of both Δf_{sw} and f_m. Thus $t_0 = 0.35T_m$ can be optimal only for one set of Δf_{sw} and f_m values (e.g. for $\Delta f_{sw} = 5$ kHz and $f_m = 500$ Hz), but for the other set of values of the parameters, it can even worsen EMI attenuation and be less effective than traditional ramp modulating waveform. Therefore optimization of MRMW is necessary. Lack of the theoretical analysis in [8] does not give a possibility to calculate optimum values of t_0 to get maximum EMI attenuation. Thus the main aim of the paper is to make the theoretical analysis of EMI spectrum and its attenuation due to the use of MRMW and propose a procedure for optimum t_0 values calculation in order to get full benefits from the use of MRMW for EMI reduction in SFM SPC.

The paper is organized as follows. In the section 2 effect of SFM on conducted EMI of boost converter is theoretically analyzed in details. In the section 3 theoretical analysis of conducted EMI and attenuation due to the use of MRMW is presented, expressions to calculate EMI spectrum are derived and procedure to calculate optimum t_0 values is proposed. In the section 4 experimental verification of the theoretical results is performed. And finally, in the section 5 conclusions are given.

2. Effect of SFM on Conducted EMI

In the analysis boost DC-DC converter operating in continuous conduction mode will be used (Fig. 1). Since for conducted EMI measurements line impedance stabilization network (LISN) is used, it will be taken into account. To simplify the analysis several assumptions will be considered:

- conducted EMI dominates at lower frequencies, because fundamental switching frequency harmonic amplitude is more pronounced than others [5], [10],

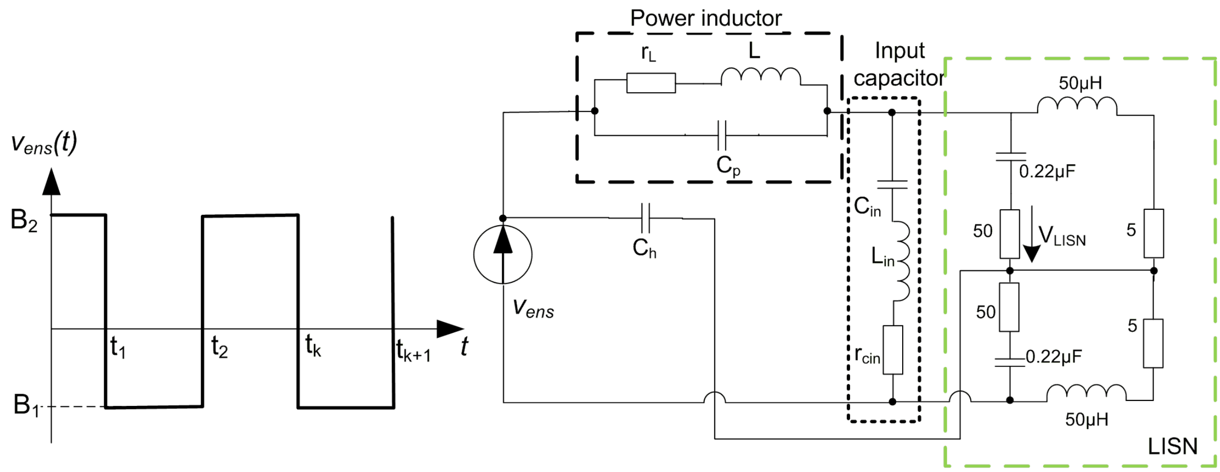

Fig. 2: Simple boost SPC model. For boost SPC: $B_1 = -V_{in}$; $B_2 = V_{out} - V_{in}$. Note the model is modified version taken from [11].

- conducted EMI levels are the highest when duty ratio D of control signal is 50 % [3],
- inductor, power switch and diode voltages are of rectangular shape.

Considering the assumptions described above, simple EMI model [11] can be used as shown in Fig. 2. The model can be used up to several MHz. For higher frequencies more complex models (taking into account other non-idealities) should be used. Using the model the transfer function between equivalent noise source V_{ens} and V_{LISN} can be derived [9]:

$$K_{EMI}(f) = \\ = \frac{50}{50 + Z_{C5}} \cdot \left(\frac{Z_e}{Z_{Ch} + Z_e} - \frac{Z_{Cin}}{2\left(Z_{Cin} + Z_L\right)} \right), \tag{1}$$

where $Z_e = (25 + Z_{C5}/2)(5 + Z_{L3})/(55 + Z_{C5} + Z_{L3})$; $Z_{C5} = 1/(j2\pi f C_5)$; $Z_{Ch} = 1/(j2\pi f C_h)$; $Z_{L3} = j2\pi f L_3$; C_h is parasitic capacitance between MOSFET drain and grounded heatsink; Z_{Cin} is real input capacitor complex impedance and Z_L is real power inductor complex impedance.

If f_{sw0}/f_m is an integer number then period of SFM voltage or current equals modulation waveform period T_m. In this case complex Fourier series coefficients for SFM V_{ens} (Fig. 2) can be derived as follows:

$$d_{sn} = -\frac{B_1}{j2\pi n} \sum_{i=1}^{N/2} \left[e^{-j2\pi n f_m t_{2i}} - e^{-j2\pi n f_m t_{2i-1}} \right] \\ - \frac{B_2}{j2\pi n} \sum_{i=1}^{N/2} \left[e^{-j2\pi n f_m t_{2i+1}} - e^{-j2\pi n f_m t_{2i}} \right], \tag{2}$$

where an integer number $N = 2f_{sw0}/f_m$; time instants t_k at which V_{ens} crosses zero (Fig. 2) can be calculated by solving the equation [12]:

$$\cos\left(2\pi f_{sw0} t + \theta(t)\right) = 0, \tag{3}$$

where time-dependent phase angle [3]:

$$\theta(t) = 2\pi \int_0^t \Delta f_{sw} \cdot m(\tau) d\tau. \tag{4}$$

By solving Eq. (3) simple expression to calculate t_k can be derived. For example, for sawtooth SFM it is [9]:

$$t_k = \frac{-f_{sw\,\min} + \sqrt{f_{sw\,\min}^2 + \Delta f_{sw}(2k-1)/T_m}}{2\Delta f_{sw}/T_m}, \tag{5}$$

where minimum switching frequency $f_{sw\,\min} = f_{sw0} - \Delta f_{sw}$; modulation index $\beta = \Delta f_{sw}/f_m$; T_m is $m(t)$ period.

In general f_{sw0}/f_m is not an integer number. In this case period of SFM voltage or current does not equal T_m but it equals KT_m, where positive integer K can be calculated as follows:

$$K = \frac{F}{f_{sw0} \cdot T_m}, \tag{6}$$

where F and K are least positive integers. Let us consider two examples:

- if $f_{sw0} = 80$ kHz and $f_m = 1$ kHz ($T_m = 1$ ms), then $K = 1$, $F = 80$ and SFM signal period is $T_m = 1$ ms,
- if $f_{sw0} = 80$ kHz and $f_m = 3$ kHz ($T_m = 1/3$ ms), then $K = 3$, $F = 80$ and SFM signal period is $3T_m = 1$ ms.

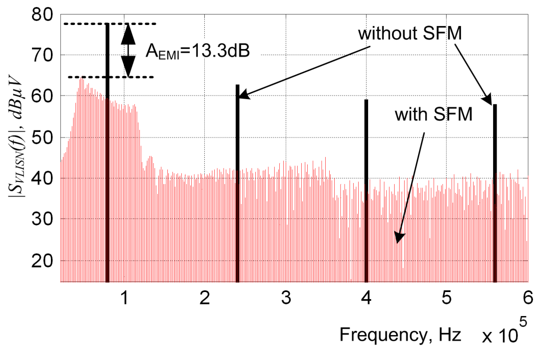

Fig. 3: V_{LISN} spectra before and after the use of SFM with sawtooth $m(t)$. Parameters: $f_m = 1$ kHz; $\Delta f_{sw} = 40$ kHz; $f_{sw0} = 80$ kHz; $C_h = 10$ pF; $V_{in} = 4$ V.

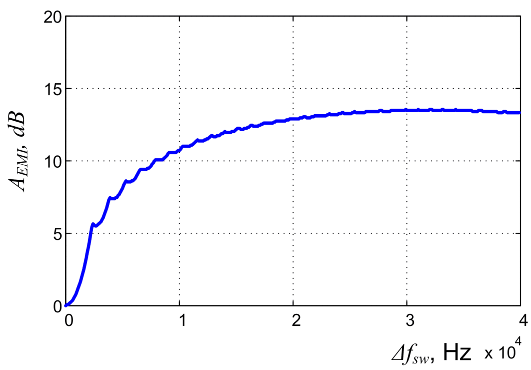

Fig. 4: A_{EMI} versus Δf_{sw}. Modulation waveform: sawtooth.

In general case (when f_{sw0}/f_m is not an integer) complex Fourier series coefficients for SFM V_{ens} can be calculated using the following expression:

$$\begin{aligned} d_{sn} &= \\ &= -\frac{B_1}{j2\pi n}\sum_{i=1}^{F}\left[e^{-j2\pi n\frac{f_m}{K}t_{2i}} - e^{-j2\pi n\frac{f_m}{K}t_{2i-1}}\right] \\ &-\frac{B_2}{j2\pi n}\sum_{i=1}^{F}\left[e^{-j2\pi n\frac{f_m}{K}t_{2i+1}} - e^{-j2\pi n\frac{f_m}{K}t_{2i}}\right]. \end{aligned} \tag{7}$$

In order to calculate V_{LISN} (conducted EMI) spectrum the following Eq. (8) can be used

$$|S_{VLISN}(f)| = 2\left|d_{sn}K_{EMI}\left(\frac{f_m n}{K}\right)\right|, \tag{8}$$

where $n = 1, 2, 3 \ldots$

As an example calculated V_{LISN} spectra of boost SPC with and without SFM are shown in Fig. 3. SFM leads to EMI spectrum spreading and in its turn to EMI attenuation. The attenuation (A_{EMI}) which is the difference in dB between maximum amplitude of unmodulated and SFM conducted EMI spectra in the frequency range of interest can be calculated as follows [9], [13]:

$$A_{EMI} = 20\log_{10}\left(\frac{\max|S_{VLISN}(f)|}{\max|S_{VLISN1}(f)|}\right), \tag{9}$$

where S_{VLISN} and S_{VLISN1} are unmodulated and SFM V_{LISN} spectra. As an example, calculated A_{EMI} versus Δf_{sw} is shown in Fig. 4.

3. Improving EMI Attenuation Using Optimization of MRMW

Fundamental switching frequency sideband can become highly asymmetrical with respect to f_{sw0} (Fig. 3) due to parasitic amplitude modulation of SPC currents [8], [9]. As it is proved in [8], [9] this leads to degradation of benefits of SFM because EMI attenuation is lower than it is expected for the given set of values of Δf_{sw} and f_m. In order to increase effectiveness of the use of SFM for EMI reduction in SPC (especially for higher values of Δf_{sw}), multislope ramp modulating waveform (MRMW) can be used [8].

3.1. Theoretical Analysis of MRMW

In this subsection comprehensive theoretical analysis of MRMW for conducted EMI reduction in boost SPC will be done.

As it can be seen from Fig. 5 slopes of the MRMW are set by parameter t_0. V_{LISN} spectrum can be calculated using Eq. (7) and Eq. (8). However it should be noted that in the case of MRMW (when $t_0 \neq 0.5T_m$) central switching frequency is:

$$f_{sw01} = f_{sw0} + \left(0.5 - \frac{t_0}{T_m}\right)\Delta f_{sw}. \tag{10}$$

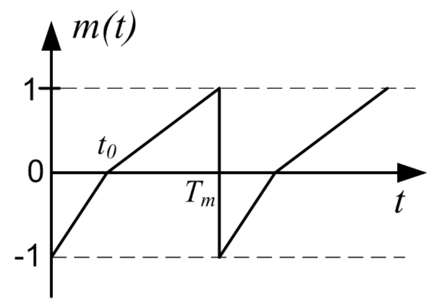

Fig. 5: MRMW.

Time instants t_K at which V_{ens} crosses zero (Fig. 2) can be calculated by solving the following Eq. (11):

$$\cos\left(2\pi f_{sw01}t + \theta(t)\right) = 0, \tag{11}$$

where time dependent phase angle can be derived using Eq. (4) as follows:

$$\theta(t) = 2\pi\Delta f_{sw} \begin{cases} \int_b^t \left(\frac{\tau - b}{t_0} - 1 - a\right) d\tau & \text{if } b \le t \le t_0 + b \\ -t_0\left(\frac{1}{2} + a\right) + \int_{t_0+b}^t \left(\frac{\tau - b - t_0}{T_m - t_0} - a\right) d\tau & \text{if } t_0 + b < t \le T_m p \end{cases}$$
$$= 2\pi\Delta f_{sw} \begin{cases} \frac{t^2}{2t_0} - t(1 + a + \frac{b}{t_0}) + \frac{b^2}{2t_0} + b(a+1) & \text{if } b \le t \le t_0 + b \\ -\frac{1}{2}t_0 + ab + \frac{t^2 + (t_0+b)^2}{2(T_m - t_0)} - t\left(\frac{t_0 + b}{T_m - t_0} + a\right) & \text{if } t_0 + b < t \le T_m p \end{cases} \tag{12}$$

where $a = 0.5 - t_0/T_m;\ b = T_m(p-1);\ p$ is modulation period number$(p = 1, 2, 3 \ldots K)$.

Following the derivations given in App. A, time instants t_k can be derived as follows

$$t_k = \begin{cases} \frac{-b_1 + \sqrt{b_1^2 - 4a_1c_1}}{2a_1} & T_m(p-1) \le t \le t_0 + T_m(p-1) \\ \frac{-b_2 + \sqrt{b_2^2 - 4a_2c_2}}{2a_2} & t_0 + T_m(p-1) < t \le T_m p \end{cases}, \tag{13}$$

where $b_1 = f_{sw01} - \Delta f_{sw}(1 + a + b/t_0)$; $a_1 = \Delta f_{sw}/(2t_0)$; $c_1 = \frac{1}{4} - \frac{k}{2} + \Delta f_{sw}\left(\frac{T_m^2(p-1)^2}{2t_0} + T_m(p-1)(a+1)\right)$; $b_2 = f_{sw01} - \Delta f_{sw}\left(\frac{t_0 + T_m(p-1)}{T_m - t_0} + a\right)$; $a_2 = \frac{\Delta f_{sw}}{2(T_m - t_0)}$; $c_2 = \frac{1}{4} - \frac{k}{2} + \Delta f_{sw}\left(\frac{(t_0 + T_m(p-1))^2}{2(T_m - t_0)} + aT_m(p-1) - \frac{1}{2}t_0\right)$.

V_{LISN} spectra and EMI attenuation due to the use of MRMW can be calculated using Eq. (7), Eq. (8), Eq. (9), Eq. (10), Eq. (11), Eq. (12), Eq. (13). For all the calculations Matlab® software is used. As an example A_{EMI} as a function of both t_0/T_m and Δf_{sw} for $f_m = 1$ kHz is shown in Fig. 6. But in Fig. 7 A_{EMI} as a function of t_0/T_m for different values of f_m is also shown. Presented results clearly show that optimum t_0 for which EMI attenuation is maximum is function of both Δf_{sw} and f_m. That is why for a given set of Δf_{sw} and f_m values optimum t_0 value should be found. For example, if $f_m = 1$ kHz and $\Delta f_{sw} = 40$ kHz, then (according to Fig. 7) optimum value of t_0 is 0.23 and maximum A_{EMI} is 16.8 dB; if $f_m = 10$ kHz and $\Delta f_{sw} = 40$ kHz, then (according to Fig. 7) optimum value of t_0 is 0.34 and maximum A_{EMI} is 7.5 dB.

3.2. MRMW Optimization Procedure

In order to get full benefits from the use of MRMW for EMI reduction procedure for optimum t_0 value calculations is to be proposed. The optimization procedure can be used not only for boost converter with different specifications but also for other power converter topologies. Since f_m and Δf_{sw} can affect not only EMI attenuation, but also other SPC parameters, such as peak-to-peak output voltage ripples, then recommendations for the choice of f_m and Δf_{sw} values proposed in [8], [14] will be taken into account in the procedure.

The MRMW optimization procedure is as follows:

- choose f_m slightly higher than RBW (resolution bandwidth) of a spectrum or EMI analyzer [8],
- choose Δf_{sw} lower than Δf_{swcr} at which peak-to-peak output voltage ripples are equal to maximally allowable values [14],
- derive conducted EMI equivalent circuit model (with LISN),
- derive analytic expression for complex transfer function $\underline{K}_{EMI}(f)$ between equivalent noise source V_{ens} and V_{LISN},
- calculate values of B_1 and B_2 for V_{ens},
- change t_0 with a small step (e.g. 0.01), and using Eq. (7), Eq. (8), Eq. (9), Eq. (10), Eq. (11), calculate V_{LISN} spectrum and A_{EMI} for each value of t_0 in the range $0.1 - 0.9$,
- find global maximum for all A_{EMI} values calculated in the previous step and find optimum t_0 for which A_{EMI} is maximum,
- end.

For determining optimized t_0 value Matlab software algorithm has been implemented. Matlab code for the optimization procedure is shown in App. B.

In order to show usefulness of the optimization procedure proposed, let us consider one example. Let us assume that we have boost converter with the following specifications: $V_{in} = 4 \ldots 8$ V, $D_{\max} = 50$ %,

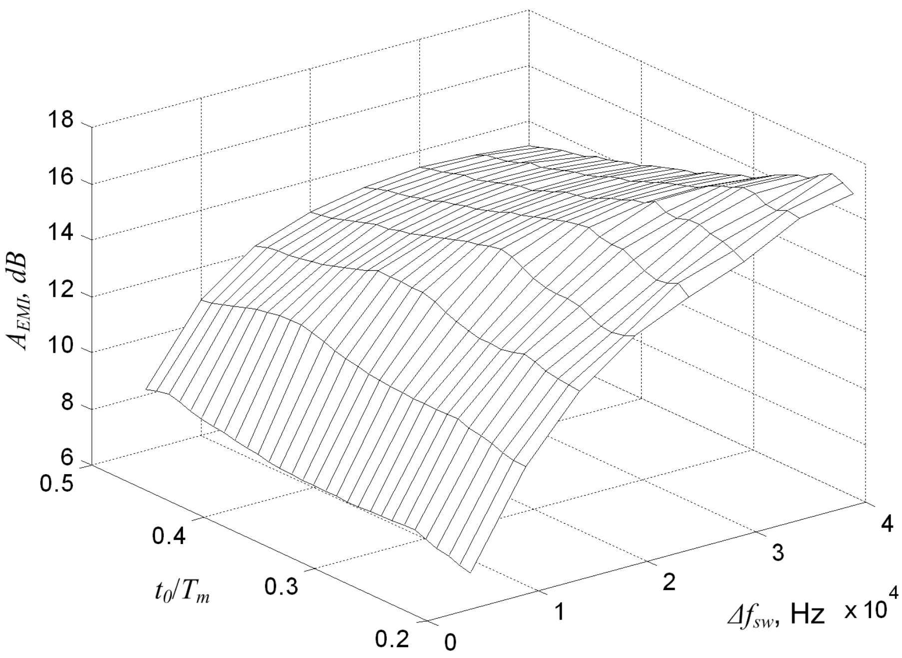

Fig. 6: Theoretically calculated A_{EMI} as a function of Δf_{sw} and t_0 Parameters: $f_m = 1$ kHz; $f_{sw0} = 80$ kHz.

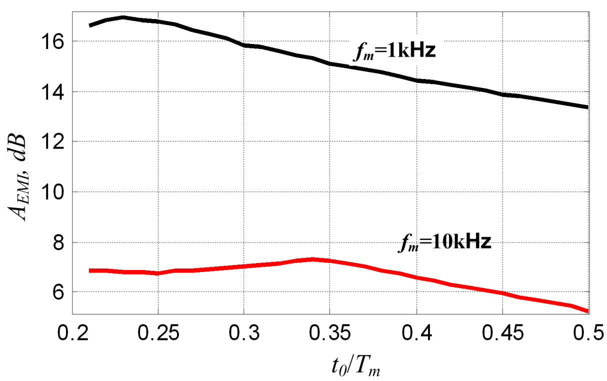

Fig. 7: Theoretically calculated A_{EMI} as a function of t_0/T_m for different f_m Parameters: $\Delta f_{sw} = 40$ kHz and $f_{sw0} = 80$ kHz.

$P_{out\,\max} = 20$ W, $f_{sw0} = 80$ kHz, $L = 40$ µH, $C_{in} = 330$ µF, $C_{out} = 1000$ µF, output capacitor equivalent series resistance (ESR) $r_{Cout} = 0.033$ Ω, output load minimum resistance $R_{out} = 12$ Ω, maximally allowable peak-to-peak output voltage ripple value $V_{pp\,\max} = 150$ mV. Let us assume that our task is to improve conducted EMI attenuation using optimized MRMW according to CISPR16 in Band A.

3.3. Solution

1) 1st Step: Choice of f_m

Since CISPR16 in Band A requires conducted EMI measurements to be done with RBW = 200 Hz and f_m should be higher than RBW, let us choose $f_m = 1$ kHz.

2) 2nd Step: Choice of Δf_{sw}

According to the procedure Δf_{sw} should be lower than Δf_{swcr} at which $V_{pp\,\max}$ are equal to maximally allowable values. In order to calculate Δf_{swcr} expression for the $V_{pp\,\max}$ calculation should be derived. The expression for the boost converter is as follows [15]

$$V_{pp\,\max} = \left(\frac{V_{in\,\max}}{(1-D_{\max})^2 R_{out}} + \frac{V_{in\,\max} D_{\max}}{2 f_{sw} L}\right) r_{Cout} + \\ + \frac{V_{in\,\max} D_{\max}}{(1-D_{\max}) R_{out} C_{out} f_{sw}}. \tag{14}$$

If f_{sw} is modulated then $f_{sw\,\min} = f_{sw0} - \Delta f_{swcr}$ should be substituted in Eq. (14) instead of f_{sw}. It can be derived that

$$\Delta f_{swcr} = f_{sw0} - \\ \frac{\frac{V_{in\,\max} D_{\max} r_{Cout}}{2L} + \frac{V_{in\,\max} D_{\max}}{(1-D_{\max}) R_{out} C_{out}}}{V_{pp\,\max} - \frac{V_{in\,\max} r_{Cout}}{(1-D_{\max})^2 R_{out}}}. \tag{15}$$

From Eq. (15) it can be obtained that $\Delta f_{swcr} = 40.4$ kHz. So Δf_{sw} is chosen to be 40 kHz.

3) 3rd Step

Boost converter conducted EMI equivalent circuit model (with LISN) is derived as shown in Fig. 2.

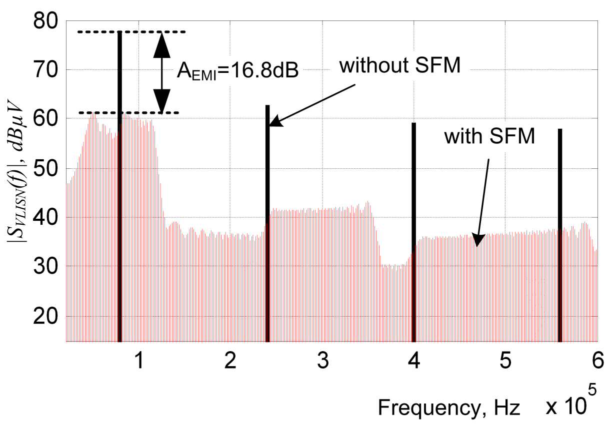

Fig. 8: V_{LISN} spectra before and after the use of SFM with optimized MRMW ($t_0 = 0.23T_m$). Other modulation and circuit parameters: the same as in Fig. 3. Note: V_{LISN} spectrum when non-optimized ramp modulation waveform is used is shown in Fig. 3.

4) 4th Step

Analytic expression for complex transfer function $\underline{K}_{EMI}(f)$ between equivalent noise source V_{ens} and V_{LISN} is derived according to Eq. (1).

5) 5th Step

$B_1 = -V_{in}$; $B_2 = V_{out} - V_{in}$.

6) Final step

Using Matlab code shown in App. B optimum t_0 is calculated to be 0.23.

V_{LISN} spectrum after the optimization of MRMW is shown in Fig. 8. As it can be seen from Fig. 3, Fig. 8 and Fig. 13d the use of optimized MRMW gives

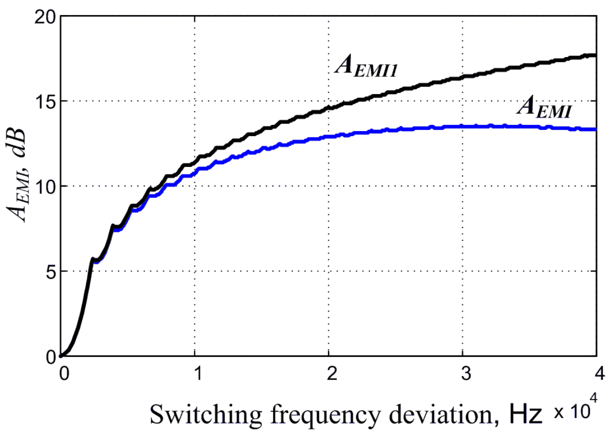

Fig. 9: Calculated A_{EMI} (when $t_0 = 0.5T_m$) and A_{EMI1} (when optimum t_0 is used) as a function of Δf_{sw} for $f_m = 1$ kHz and $f_{sw0} = 80$ kHz.

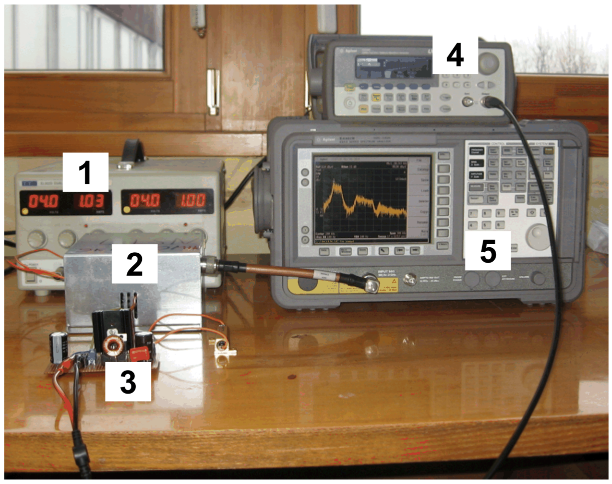

Fig. 10: Experimental setup picture. **1** DC power source TTI EL302D; **2** DC LISN (homemade); **3** boost converter under test; **4** arbitrary waveform generator Agilent 33220A; **5** spectrum analyzer Agilent E4402B.

3.5 dB better A_{EMI} than the use of conventional ramp modulation waveform (when $t_0 = 0.5T_m$) and 1.7 dB better A_{EMI} than the use of MRMW proposed in [8] (when $t_0 = 0.35T_m$). Comparison of A_{EMI} versus Δf_{sw} for conventional ramp modulation waveform and optimized MRMW is depicted in Fig. 9. The results clearly show that optimized MRMW is more useful for higher Δf_{sw}.

4. Experimental Verification

4.1. Experimental Setup

For the experimental verifications a low power SFM boost SPC is used (Fig. 11). The converter operates in open-loop continuous conduction mode. Duty ratio D and input voltage of the converter can be varied. However in the experiments duty ratio of 50 % is chosen because from conducted EMI point of view it is the worst situation [3]. Input DC voltage of the

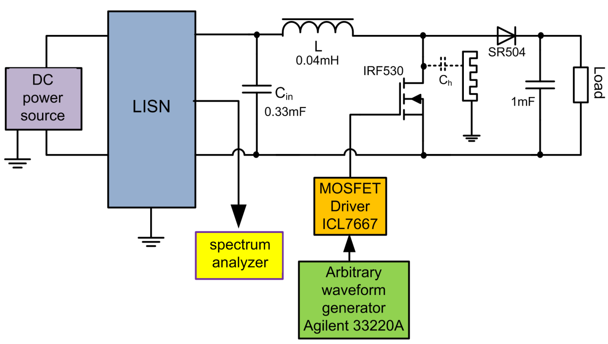

Fig. 11: Simplified schematic diagram of the experimental setup.

converter can be changed from 2 V to 8 V. Nominal switching frequency is 80 kHz. Nominal output power is 20 W. In the experiments power MOSFET is used with grounded external heatsink. Measured parasitic capacitance C_h between MOSFET drain and ground is of about 10 pF. Arbitrary waveform generator (AWG) Agilent 33220A controls the power MOSFET via MOSFET driver ICL7667. The control signal of the power MOSFET can be both unmodulated and switching frequency modulated. All the necessary SFM parameters (including t_0) can be set using the AWG which has built-in frequency modulator and waveform editor. MRMW with custom t_0 can be obtained using the waveform editor. Figure 12 depicts the photo of the AWG Agilent 33220A front panel and display.

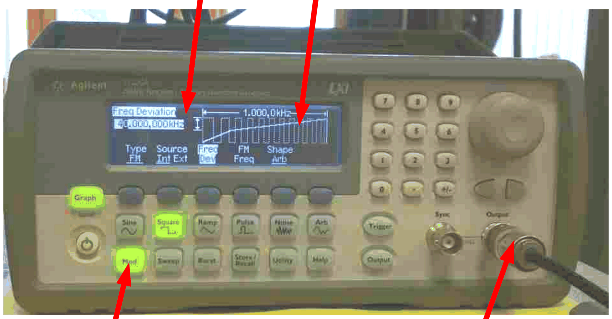

Fig. 12: AWG front panel and waveform editor display photo.

4.2. Experimental Results

Conducted EMI (V_{LISN} spectrum) is measured using Agilent E4402B spectrum analyzer with RBW=200 Hz and peak detector. Experiments have been done for different V_{in} and output power values. Comparison of the experimental and the theoretical V_{LISN} spectra when $V_{in} = 4$ V and $D = 50$ % is presented in Fig. 13. Experiments revealed that changing input voltage and output load does not have any noticeable influence on EMI attenuation and optimized t_0 value. Experimental results confirm theoretical predictions that the use of optimized MRMW can noticeably increase EMI attenuation: the use of optimized MRMW gives 3.8 dB better A_{EMI} than the use of conventional ramp modulation waveform (when $t_0 = 0.5T_m$) and 2 dB better A_{EMI} than the use of MRMW proposed in [8] (when $t_0 = 0.35T_m$). Experimental and theoretical results are in a good agreement: when Δf_{sw} was increased to 40 kHz, experimental EMI attenuation increased to 16.9 dB, but theoretical one to 16.8 dB.

5. Conclusion

Comprehensive theoretical analysis of SPC conducted EMI spectrum and attenuation presented in the paper shows that the use of multislope ramp modulation waveform can noticeably improve EMI reduction in switching-frequency-modulated switching power converters. However in order to get full benefits from the use of MRMW, optimum value of the parameter t_0 which controls the slopes of the waveform should be found. For this purpose the optimization procedure has been proposed and usefulness of the procedure has been verified experimentally using boost SPC. The procedure is based on the analytic expressions derived for conducted EMI spectrum and attenuation calculation. It has been shown that optimum value of parameter t_0 is the function of switching frequency deviation and modulation frequency.

Acknowledgment

Support for this work was provided by the Riga Technical University through the Scientific Research Project Competition for Young Researchers No. ZP-2014/9.

References

[1] MAINALI, K. and R. ORUGANTI. Conducted EMI Mitigation Techniques for Switch-Mode Power Converters: A Survey. *IEEE Transactions on Power Electronics*. 2010, vol. 25, iss. 9, pp. 2344–2356. ISSN 0885-8993. DOI: 10.1109/TPEL.2010.2047734.

[2] YAZDANI, M. R., H. FARZANEHFARD and J. FAIZ. Classification and Comparison of EMI Mitigation Techniques in Switching Power Converters - A review. *Journal of Power Electronics*. 2011, vol. 11, iss. 5, pp. 767–777. ISSN 1598-2092.

[3] GONZALEZ, D., J. BALCELLS, A. SANTOLARIA, J.-C LE BUNETEL, J. GAGO, D. MAGNON and S. BREHAUT. Conducted EMI Reduction in Power Converters by Means of Periodic Switching Frequency Modulation. *IEEE Transactions on Power Electronics*. 2007, vol. 22, iss. 6, pp. 2271–2281. ISSN 0885-8993. DOI: 10.1109/TPEL.2007.909257.

[4] HAMZA, D. and M. QIU. Digital Active EMI Control Technique for Switch Mode Power Converters. *IEEE Transactions on Electromagnetic Compatibility*. 2013, vol. 55, iss. 1, pp. 81–88. ISSN 0018-9375. DOI: 10.1109/TEMC.2012.2213590.

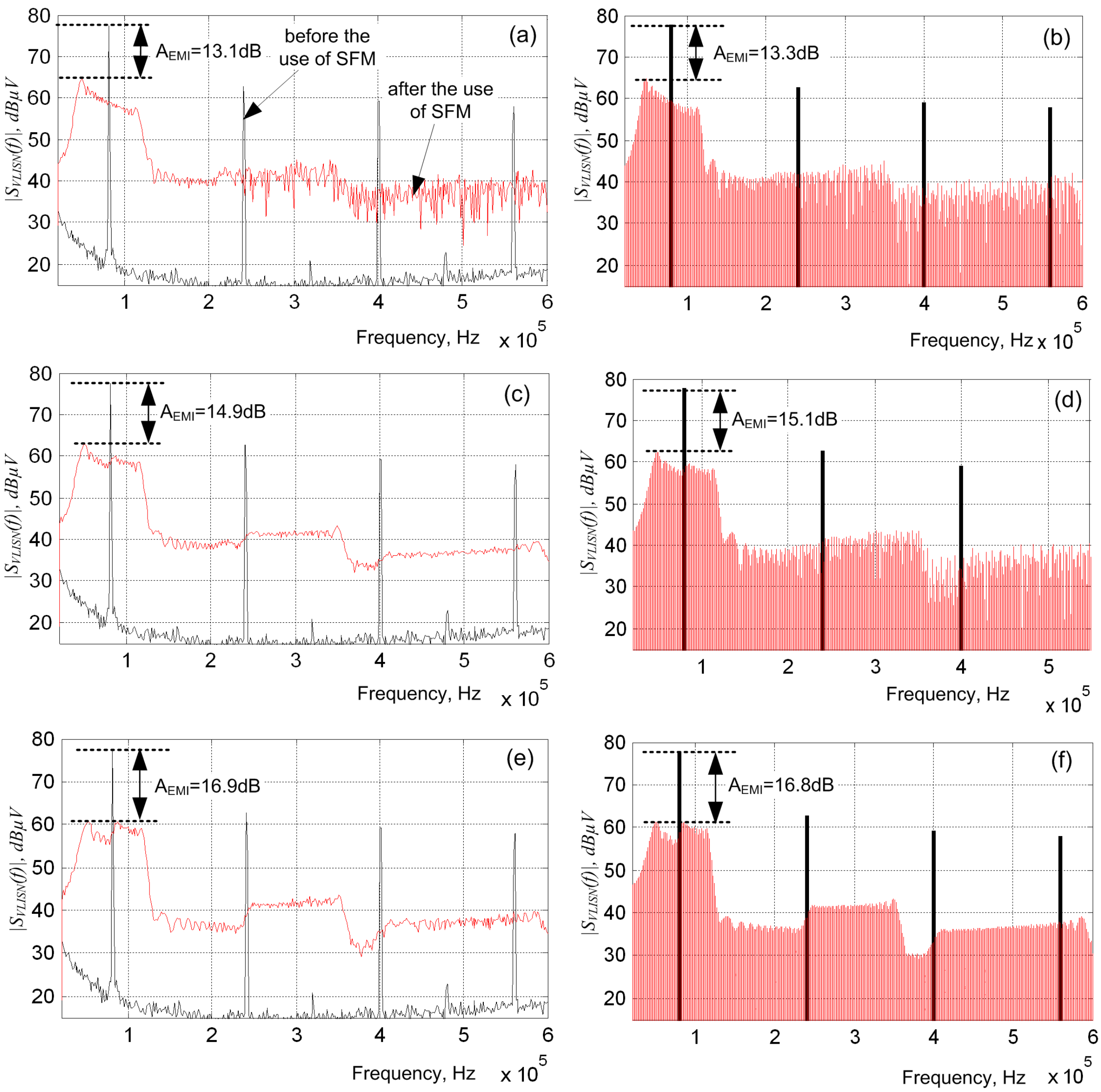

Fig. 13: Experimental (a), (c), (e) and theoretical (b), (d), (f) conducted EMI spectra in the frequency range 20 – 600 kHz: (a), (b) conventional ramp ($t_0 = 0.5T_m$); (c), (d) modified ramp proposed in [8] ($t_0 = 0.35T_m$); (e), (f) optimized MRMW propsed in this paper (optimum $t_0 = 0.23T_m$). Spectrum analyzer parameters: RBW=200 Hz; peak detector. SPC and SFM parameters: $V_{in} = 4$ V; $D = 0.5$; $f_{sw0} = 80$ kHz; $f_m = 1$ kHz; $\Delta f_{sw} = 40$ kHz; $C_h = 10$ pF.

[5] CABUK, G. and S. KILINC. Reducing electromagnetic interferences in flyback AC-DC converters based on the frequency modulation technique. *Turkish Journal of Electrical Engineering & Computer Sciences*. 2012, vol. 20, iss. 1, pp. 71–86. ISSN 1300-0632.

[6] TSE, K., H. CHUNG, R. NG and R. HUI. An Evaluation of the Spectral Characteristics of Switching Converters with Chaotic-Frequency Modulation. *IEEE Transactions on Industrial Electronics*. 2003, vol. 50, iss. 1, pp. 171–181. ISSN 0278-0046. DOI: 10.1109/TIE.2002.807659.

[7] JANKOVSKIS, J., D. STEPINS, S. TJUKOVS and D. PIKULINS. Examination of Different Spread Spectrum Techniques for EMI Suppression in dc/dc Converters. *Electronics and Electrical Engineering*. 2008, vol. 86, iss. 6, pp. 60–64. ISSN 1392-1215.

[8] JOHNSON, S. and R. ZANE. Custom spectral shaping for EMI reduction in high-frequency inverters and ballasts. *IEEE Transactions on Power Electronics*. 2005, vol. 20, iss. 6, pp. 1499–1505. ISSN 0885-8993. DOI: 10.1109/TPEL.2005.857565.

[9] STEPINS, D. Conducted EMI of Switching Frequency Modulated Boost Converter. *Electrical,*

Control and Communication Engineering. 2013, vol. 3, iss. 1, pp. 12–18. ISSN 2255-9159. DOI: 10.2478/ecce-2013-0009.

[10] BALCELLS, J., D. GONZALES, J. GAGO, A. SANTOLARIA, J.-C. LE BUNETEL, D. MAGNON and S. BREHAUT. Frequency modulation techniques for EMI reduction in SMPS. In: *Proceedings of the 9th European Conference on Power Electronics and Applications*. Dresden: IEEE, 2005, pp. 1–8. ISBN 90-75815-09-3. DOI: 10.1109/EPE.2005.219198.

[11] MUSZNICKI, P., J.-L. SCHANEN, P. GRANJON and P. CHRZAN. Better understanding EMI generation of power converters. In: *Proceedings of IEEE Power Electronics Specialists Conference (PESC2005)*. Recife: IEEE, 2005, pp. 1052–1056. ISBN 0-7803-9033-4. DOI: 10.1109/PESC.2005.1581758.

[12] HARDIN, K., J. FESSLER and D. BUSH. Spread Spectrum Clock Generation for the Reduction of Radiated Emissions. In: *Proceedings of IEEE International Symposium on Electromagnetic Compatibility*. Chicago: IEEE, 1994, pp. 227-231. ISBN 0-7803-1398-4. DOI: 10.1109/ISEMC.1994.385656.

[13] BARRAGAN, L., D. NAVARRO, J. ACERO, I. URRIZA and J. BURDIO. FPGA Implementation of a Switching Frequency Modulation Circuit for EMI Reduction in Resonant Inverters for Induction Heating Appliances. *IEEE Transactions on Industrial Electronics*. 2008, vol. 55, iss. 1, pp. 11–20. ISSN 0278-0046. DOI: 10.1109/TIE.2007.896129.

[14] STEPINS, D. Effect of frequency modulation on input current of switch-mode power converter. In: *Proceedings of 39th Annual Conference of the IEEE Industrial Electronics Society, IECON 2013*. Vienna: IEEE, 2013, pp. 683–688. ISBN 978-1-4799-0224-8. DOI: 10.1109/IECON.2013.6699217.

[15] HAUKE, B. Basic calculation of a boost converter's power stage. In: *Texas Instruments: Application Report* [online]. 2009. Available at: `http://www.ti.com/lit/an/slva372c/slva372c.pdf`.

About Authors

Deniss STEPINS received the B.Sc., M.Sc. (with honors) and Dr.Sc.ing degrees in electronics from Riga Technical University, Riga, Latvia, in 2004, 2006 and 2011 respectively. He is currently a senior research fellow and lecturer in the Institute of Radio Electronics, Riga Technical University. He has been involved in several research projects on examination of spread spectrum technique for switching power converters, improvement of power magnetic components and EMI filter optimization. His research interests include EMI reduction techniques applied to switching power converters, control of switch-mode power converters, planar magnetic components and three-phase EMI filters. He is currently an IEEE and an IEEE Industrial Electronics Society member.

Jin HUANG received the B.Sc. degree from Shanghai Jiaotong University, Shanghai, China, in 1992, and the M.Sc. and Ph.D. degrees from the Huazhong University of Science and Technology, Wuhan, China, in 2003 and 2009, respectively. In 2000, he joined Huazhong University of Science and Technology as a Lecturer. He is currently an Associate Professor in the School of Electrical and Electronic Engineering. His research interests include the control technique, EMC and reliability of power electronics devices.

Appendix A Derivation of Eq. (13)

By substituting Eq. (10) and Eq. (12) into Eq. (11) the following trigonometric equations can be obtained

$$\begin{cases} \cos\left[2\pi f_{sw01}t + 2\pi\Delta f_{sw}\left(\frac{t^2}{2t_0} - t\left(1+a+\frac{b}{t_0}\right) + \frac{b^2}{2t_0} + b(a+1)\right)\right] = 0 \\ \text{if } b \le t \le t_0 + b, \\ \\ \cos\left[2\pi f_{sw01}t + 2\pi\Delta f_{sw}\left(-\frac{1}{2}t_0 + ab + \frac{t^2+(t_0+b)^2}{2(T_m-t_0)} - t\left(\frac{t_0+b}{T_m-t_0}+a\right)\right)\right] = 0 \\ \text{if } t_0 + b < t \le T_m p. \end{cases} \tag{A1}$$

Assuming that $\arccos(0) = -\pi/2 + \pi k$, where $k = 1, 2, 3\ldots$, the following equation can be obtained from Eq. (A1).

$$\begin{cases} 2\pi f_{sw01}t + 2\pi\Delta f_{sw}\left(\frac{t^2}{2t_0} - t\left(1+a+\frac{b}{t_0}\right) + \frac{b^2}{2t_0} + b(a+1)\right) = -\frac{\pi}{2} + \pi k \\ \text{if } b \le t \le t_0 + b, \\ \\ 2\pi f_{sw01}t + 2\pi\Delta f_{sw}\left(-\frac{1}{2}t_0 + ab + \frac{t^2+(t_0+b)^2}{2(T_m-t_0)} - t\left(\frac{t_0+b}{T_m-t_0}+a\right)\right) = -\frac{\pi}{2} + \pi k \\ \text{if } t_0 + b < t \le T_m p. \end{cases} \tag{A2}$$

From Eq. (A2) one can get the following quadratic equations

$$\begin{cases} \frac{\Delta f_{sw}}{2t_0}t^2 + \left(f_{sw01} - \Delta f_{sw}\left(1+a+\frac{b}{t_0}\right)\right)t + \left(\frac{1}{4} - \frac{k}{2} + \Delta f_{sw}\left(\frac{b^2}{2t_0} + b(a+1)\right)\right) = 0 \\ \text{if } b \le t \le t_0 + b, \\ \\ \frac{\Delta f_{sw}}{2(T_m-t_0)}t^2 + \left(f_{sw01} - \Delta f_{sw}\left(\frac{t_0+b}{T_m-t_0}+a\right)\right)t + \\ + \left(\frac{1}{4} - \frac{k}{2} + \Delta f_{sw}\left(\frac{(t_0+b)^2}{2(T_m-t_0)} + ab - \frac{1}{2}t_0\right)\right) = 0 \\ \text{if } t_0 + b < t \le T_m p. \end{cases} \tag{A3}$$

Finally Eq. (13) can be derived by solving Eq. (A3).

Appendix B Matlab code for optimum t_0 calculation

```
delta=40e3; % enter switching frequency deviation
fsw=80e3; % enter central switching frequency
fm=1e3; % enter modulation frequency
Tm=1/fm; K=5; Uin=4; D=0.5; % enter input voltage and duty ratio
L=40e-6; % enter power inductor inductance
Ch=10e-12; % enter parasitic capacitance Ch between MOSFET drain and ground
Cin=330e-6; Lp=10e-9; esr=0.06; % enter parameters of input capacitor
L3=50e-6; R3=5; C5=0.22e-6; % enter LISN parameters
Uout=Uin/(1-D); % calculation of output voltage

%--------------------------------------------------------------------------------
for p=1:40 % calculation of time instants tk according to Eq. (13)
t0=0.1*Tm+0.01*Tm*p;
to(p)=t0;
f=1; a1=delta/2/t0; a2=delta*0.5/(Tm-t0); a=0.5-t0/Tm; t1=0; fsw1=fsw+a*delta;
M=K*2*fsw1/fm;
for m=1:M
```

```
if t1<t0+Tm*(f-1)
  b1=fsw1-delta*(1+a+Tm*(f-1)/t0);
  c1=0.25-m/2+((Tm.^2*(f-1).^2)/2/t0+Tm*(f-1)*(a+1))*delta;
  tk(m)=(-b1+sqrt(b1.^2-4*a1*c1))./(2*a1);
  t1=(-b1+sqrt(b1.^2-4*a1*c1))./(2*a1);
if t1>t0+Tm*(f-1)
  b2=fsw1-delta*((t0+Tm*(f-1))/(Tm-t0)+a);
  c2=0.25-m/2+delta*(-0.5*t0+a*Tm*(f-1)+0.5./(Tm-t0).*(t0+Tm*(f-1)).^2);
  tk(m)=(-b2+sqrt(b2.^2-4*a2*c2))./(2*a2);
  t1=(-b2+sqrt(b2.^2-4*a2*c2))./(2*a2);
end
else
  b2=fsw1-delta*((t0+Tm*(f-1))/(Tm-t0)+a);
  c2=0.25-m/2+delta*(-0.5*t0+a*Tm*(f-1)+0.5./(Tm-t0).*(t0+Tm*(f-1)).^2);
  tk(m)=(-b2+sqrt(b2.^2-4*a2*c2))./(2*a2);
  t1=(-b2+sqrt(b2.^2-4*a2*c2))./(2*a2);
if t1>Tm*f
  f=f+1;
  b1=fsw1-delta*(1+a+Tm*(f-1)/t0);
  c1=0.25-m/2+((Tm.^2*(f-1).^2)/2/t0+Tm*(f-1)*(a+1))*delta;
  tk(m)=(-b1+sqrt(b1.^2-4*a1*c1))./(2*a1);
  t1=(-b1+sqrt(b1.^2-4*a1*c1))./(2*a1);
end
end
end
%------------------------------------------------------------------------------
%------------------------------------------------------------------------------
for  n=200:1000 %calculation of complex Fourier series coefficients dsn according
to Eq. (2)
  for i=1:M/2
    ann(i)=Uout*(exp(-j*n*2*pi*fm/K*tk(2*i))-exp(-j*n*2*pi*fm/K*(tk(2*i-1))))./
    (j*2*pi*n);
  end
an=sum(ann);

%------------------------------------------------------------------------------
w=2*pi*fm*n/K;
Z=(j*w*L3+R3).*(50+1./(j*w*C5))./2./((j*w*L3+R3+50+1./(j*w*C5)));     %enter LISN
impedance Ze
KEMI=-(1./(j*Cin*w)+esr+j*Lp*w)./(j*L*w)./2+Z./(Z+1./(j*Ch*w));  %enter KEMI from
EMI model
VLISN(n)=abs(2*an.*KEMI); %calculation of VLISN spectrum
end


Z1=(j*2*pi*fsw*L3+R3).*(50+1./(j*2*pi*fsw*C5))./2./((j*2*pi*fsw*L3+R3+50+1./
(j*2*pi*fsw*C5)));
KEMI1=-(1./(j*Cin*2*pi*fsw)+esr+j*Lp*2*pi*fsw)./(j*L*2*pi*fsw)./2+Z1./(Z1+1./
(j*Ch*2*pi*fsw));
cc1=4*Uin/pi;
VLISN1=abs(cc1.*KEMI1); %calculation of VLISN 1st harmonic amplitude without SFM


AEMI(p)=max(abs(20*log10(VLISN1./(max(VLISN))))); %calculation of AEMI vs t0
end

[x,y]=max(AEMI); %determination of max AEMI (finding global maximum)
optimumt0=to(y)./Tm %optimum t0 calculation
```